

Neutron diffraction study of the magnetic structure of the superconducting Ru-1222-type ruthenocuprate $\text{RuSr}_2\text{Y}_{1.5}\text{Ce}_{0.5}\text{Cu}_2\text{O}_{10-\delta}$: Evidence for long-range antiferromagnetic order

A. C. McLaughlin*

Department of Chemistry, University of Aberdeen, Meston Walk, Aberdeen AB24 3UE, United Kingdom

I. Felner

Racah Institute of Physics, The Hebrew University, Jerusalem 91904, Israel

V. P. S. Awana

National Physical Laboratory, Dr. K. S. Krishnan Road, New Delhi 110012, India

and ICYS, National Institute for Material Science (NIMS), Tsukuba, Ibaraki 305-0044, Japan

(Received 17 July 2007; revised manuscript received 27 June 2008; published 2 September 2008)

A neutron diffraction study on the superconducting Ru-1222 ruthenocuprate $\text{RuSr}_2\text{Y}_{1.5}\text{Ce}_{0.5}\text{Cu}_2\text{O}_{10-\delta}$ ($T_c=35$ K) prepared by the high-pressure high-temperature technique reveals long-range antiferromagnetic order below 140 K. Neighboring spins are antiparallel on the ab plane but both antiferromagnetic and ferromagnetic alignments along c are observed. The refined low-temperature moment is $1.5(3)\mu_B$. The observation of a ferromagnetic moment from magnetic measurements suggests that the Ru spins are canted below 91 K with a zero-field moment of $<0.3\mu_B$.

DOI: 10.1103/PhysRevB.78.094501

PACS number(s): 74.70.Pq, 74.25.Ha, 74.72.-h, 75.25.+z

I. INTRODUCTION

The $\text{RuSr}_2R\text{Cu}_2\text{O}_8$ (R =rare earth, Ru-1212) (Refs. 1–4) and $\text{RuSr}_2R_{2-x}\text{Ce}_x\text{Cu}_2\text{O}_{10-\delta}$ (Ru-1222) (Refs. 1, 2, and 5) type ruthenocuprates have been well studied in recent years due to the observation of coexisting weak ferromagnetism (W-FM) and superconductivity. W-FM is observed in the ruthenate layer below 100–150 K and superconductivity in copper oxide planes below $T_c \sim 50$ K. Neutron-scattering experiments on $\text{RuSr}_2\text{GdCu}_2\text{O}_8$ (Ref. 6) and $\text{Pb}_2\text{RuSr}_2\text{Cu}_2\text{O}_8\text{Cl}$ (Ref. 7) have recently shown that G -type antiferromagnetic (AFM) order is present within the RuO_2 planes. An upper limit of $0.1\mu_B$ was obtained for the ferromagnetic component. Upon application of a magnetic field, the Ru spins cant further away from the G -type magnetic structure and at 7 T the order of the Ru spins is almost fully ferromagnetic. The magnetic structure of the underdoped Ru-1222 ruthenocuprate $\text{RuSr}_2\text{Nd}_{0.9}\text{Y}_{0.2}\text{Ce}_{0.9}\text{Cu}_2\text{O}_{10-\delta}$ has recently been reported.⁸ In this material AFM ordering of both Ru and Cu moments are observed at low temperature. Neutron diffraction studies have shown that below the Ru spin ordering temperature T_{Ru} , additional peaks from a $(\frac{1}{2}\frac{1}{2}\frac{1}{2})$ magnetic superstructure are observed which can be fitted by a model of antiferromagnetically ordered Ru moments aligned in the c direction.⁸ The Cu spins order antiferromagnetically on the ab plane with a $(\frac{1}{2}\frac{1}{2}0)$ superstructure below a second transition at T_{Cu} . Upon application of a magnetic field, the Ru and Cu moments cant into a ferromagnetic alignment on the ab plane. The underdoped $\text{RuSr}_2\text{Nd}_{1.8-x}\text{Y}_{0.2}\text{Ce}_x\text{Cu}_2\text{O}_{10-\delta}$ ($0.7 \leq x \leq 0.95$) ruthenocuprates are not superconducting but exhibit large negative magnetoresistances [$\text{MR}=(\rho_H-\rho_0)/\rho_0$] at low temperature of up to -49% at 4 K in a 9 T field,^{8–11} demonstrating strong spin-charge coupling within the CuO_2 planes. MR initially rises to $\sim 2\%$ at T_{Ru} as observed in other superconducting ruthenocuprates, but increases dramatically on cooling.

The magnetotransport in Ru-1222 ruthenocuprates is also very sensitive to lattice effects. In a series of $\text{RuSr}_2R_{1.1}\text{Ce}_{0.9}\text{Cu}_2\text{O}_{10-\delta}$ (R =Nd, Sm, Eu, and Gd with Y) samples where the hole doping level is constant, the high-field MR does not correlate with the paramagnetic moment of the R cations but shows an unprecedented crossover from negative to positive MR values as $\langle r_A \rangle$, the mean A site ($R_{1.1}\text{Ce}_{0.9}$) cation radius, decreases.⁹

Although the magnetic structure of highly underdoped Ru-1222 is now known, it is still unclear as to whether long-range magnetic order of the Ru spins continues into the higher doped and superconducting regions of the phase diagram. Previous low-temperature neutron diffraction studies on superconducting $\text{RuSr}_2^{160}\text{Gd}_{1.3}\text{Ce}_{0.7}\text{Cu}_2\text{O}_{10-\delta}$ ($T_c=29$ K) (Ref. 12) and $\text{RuSr}_2^{153}\text{Eu}_{1.2}\text{Ce}_{0.8}\text{Cu}_2\text{O}_{10-\delta}$ (Ref. 13) ($T_c=40$ K) failed to reveal any magnetic intensity arising from order of the Ru spins below T_{Ru} . Furthermore the magnetic properties of polycrystalline superconducting $\text{RuSr}_2\text{Gd}_{1.5}\text{Ce}_{0.5}\text{Cu}_2\text{O}_{10-\delta}$ ($T_c=40$ K) have been studied by ac susceptibility and results demonstrate that a sharp frequency dependent peak is observed at $T_f=72$ K.¹⁴ The frequency dependence observed is typical of the dynamics of spin-glass systems and the change in the peak position with frequency follows the Vogel-Fulcher law. It was concluded that $\text{RuSr}_2\text{Gd}_{1.5}\text{Ce}_{0.5}\text{Cu}_2\text{O}_{10-\delta}$ exhibits spin-glass behavior with magnetically interacting clusters and that long-range magnetic order is not observed.¹⁴ This is in contrast to the usual interpretation of the existence of long-range magnetic order in other reports in which two magnetic transitions are observed at T_{M2} and T_M ($T_{M2} < T_M$).¹⁵ It has been suggested that below T_{M2} the Ru moments are weakly ferromagnetically ordered and that the magnetic transition at T_M may arise from the presence of nanoparticles of a minor magnetic phase $(\text{Sr,Cu})(\text{Ru,Cu})\text{O}_3$.¹⁵ In this paper results from neutron diffraction on a Ru-1222 sample, namely, $\text{RuSr}_2\text{Y}_{1.5}\text{Ce}_{0.5}\text{Cu}_2\text{O}_{10-\delta}$, with hole doping level $p \sim 2.25$ are

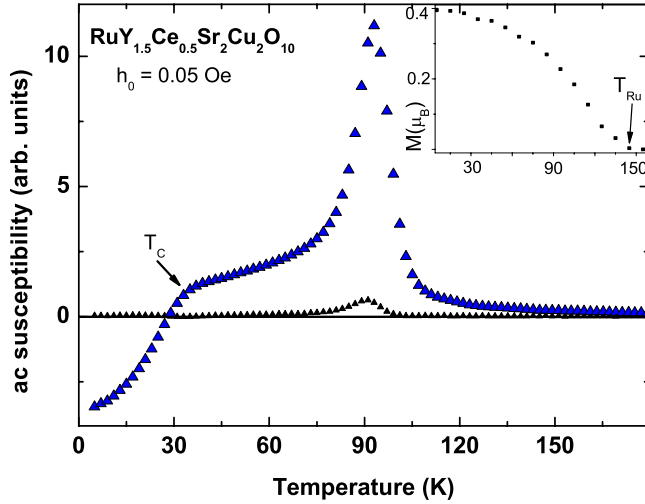


FIG. 1. (Color online) Real (top) and imaginary (bottom) ac susceptibility plots for $\text{RuSr}_2\text{Y}_{1.5}\text{Ce}_{0.5}\text{Cu}_2\text{O}_{10-\delta}$ measured at 1465 Hz. The inset exhibits the temperature dependence of the saturation moment from which T_{Ru} is deduced.

reported. Since the neutron absorption cross section of Y is negligible, $\text{RuSr}_2\text{Y}_{1.5}\text{Ce}_{0.5}\text{Cu}_2\text{O}_{10-\delta}$ is as an excellent candidate for neutron diffraction studies.

II. EXPERIMENT

$\text{RuSr}_2\text{Y}_{1.5}\text{Ce}_{0.5}\text{Cu}_2\text{O}_{10-\delta}$ was synthesized by the high-pressure high-temperature (HPHT) technique. Prescribed amounts of RuO_2 , SrO_2 , SrCuO_2 , $0.75\text{Y}_2\text{O}_3$, 0.5CeO_2 , 0.75CuO , and 0.25Cu were mixed and sealed in a gold capsule and heated at 1450°C under 6 GPa of oxygen for 3 h and quenched to room temperature and then the pressure was released. Laboratory x-ray diffraction patterns demonstrate that $\text{RuSr}_2\text{Y}_{1.5}\text{Ce}_{0.5}\text{Cu}_2\text{O}_{10-\delta}$ is phase pure. Isothermal magnetization $M(H)$ measurements up to ± 50 kOe were carried out at various temperatures in a commercial (Quantum Design) superconducting quantum interference device (SQUID) magnetometer. The ac susceptibility (at $H_{\text{dc}}=0$ and ac amplitude of 0.05 Oe) at various frequencies ($f=165\text{--}1465$ Hz) was measured by homemade probes inserted in the SQUID.

III. RESULTS AND DISCUSSION

The ac susceptibility curve (Fig. 1) shows the superconducting temperature at $T_c=35$ K and a magnetic transition at 91 K. In contrast M_{sat} , which corresponds to the magnetic contribution of the Ru sublattice, becomes zero at $T_{\text{Ru}}=140(1)$ K (Fig. 1 inset). In order to determine M_{sat} , isothermal magnetization $M(H)$ measurements were performed at various temperatures. The $M(H)$ curves below T_{Ru} are strongly dependent on the field up to 5–7 kOe until a common slope is reached. $M(H)$ can be described as $M(H) = M_{\text{sat}} + \chi H$, where χH is the linear contribution to M . Figure 2 shows a typical $M(H)$ curve recorded at 115 K. Upon closer inspection of the ac susceptibility data, it is possible to see that the susceptibility data also start to deviate at $T_{\text{Ru}}=140$ K (Fig. 3 inset), which suggests that magnetic order of

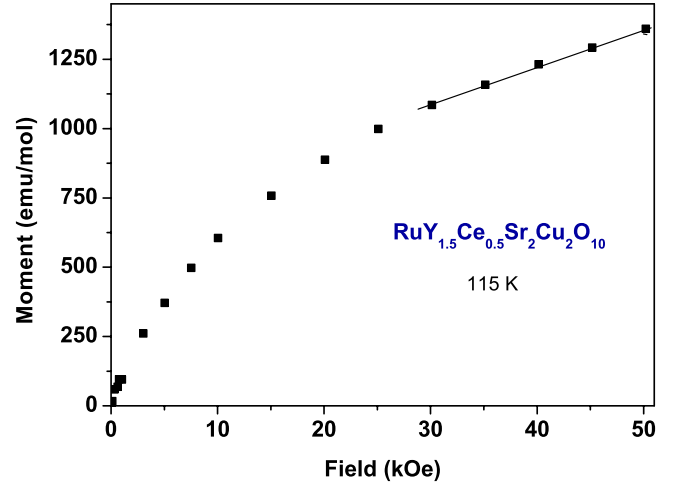


FIG. 2. (Color online) The isothermal magnetization for $\text{RuSr}_2\text{Y}_{1.5}\text{Ce}_{0.5}\text{Cu}_2\text{O}_{10-\delta}$ recorded at 115 K.

the Ru spins occurs below this temperature, followed by a different magnetic transition at 91 K. The highest $M_{\text{sat}} = 0.40\mu_B/\text{Ru}$ achieved is at 5 K. This value is much smaller than $1\mu_B$, the expected moment for Ru^{5+} in the low-spin state ($g=2$ and $S=0.5$), or $3\mu_B$ expected in the high-spin state ($g=2$ and $S=1.5$). This indicates that some canting on adjacent Ru spins occurs in the magnetically ordered state. Note that M_{sat} decreases monotonically up to T_{Ru} without any inflection around 91 K (Fig. 1 inset).

Figure 3 shows the real ac susceptibility curves measured on $\text{RuSr}_2\text{Y}_{1.5}\text{Ce}_{0.5}\text{Cu}_2\text{O}_{10-\delta}$ under an ac field of $H_{\text{ac}}=0.05$ Oe at various frequencies (f). The main peak is observed at $T_f=90.9(1)$ and within the uncertainty limit (0.1 K), no shift in the peak position is observed. This is in contrast to ac studies previously performed on $\text{RuSr}_2\text{Gd}_{1.5}\text{Ce}_{0.5}\text{Cu}_2\text{O}_{10-\delta}$, where T_f is frequency dependent, shifting to higher temperatures as f increases.¹⁴ These results demonstrate the same spin-glass behavior is not present in this sample.

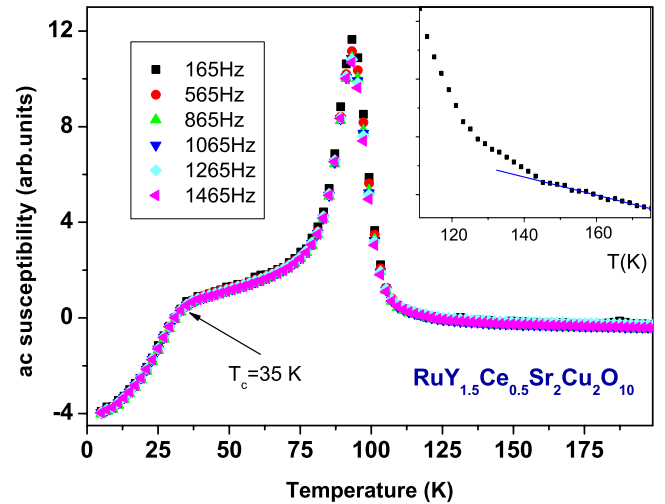


FIG. 3. (Color online) Temperature dependence of the real ac susceptibility for $\text{RuSr}_2\text{Y}_{1.5}\text{Ce}_{0.5}\text{Cu}_2\text{O}_{10-\delta}$ measured at various frequencies. The inset shows an enlarged region of the data with $f=1465$ Hz.

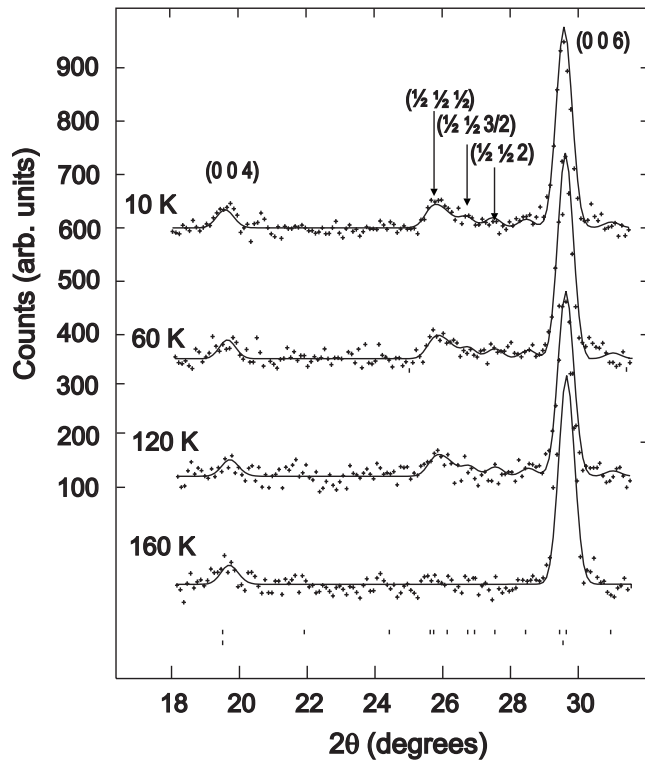


FIG. 4. Portion of the low-angle neutron diffraction pattern recorded for $\text{RuSr}_2\text{Y}_{1.5}\text{Ce}_{0.5}\text{Cu}_2\text{O}_{10-\delta}$ demonstrating the presence of weak magnetic peaks below 140 K. The top and bottom reflector markers correspond to the magnetic and structural phases, respectively.

In order to determine the magnetic structure and the magnetic transition temperature, variable-temperature neutron diffraction patterns were recorded for $\text{RuSr}_2\text{Y}_{1.5}\text{Ce}_{0.5}\text{Cu}_2\text{O}_{10-\delta}$ on the high intensity instrument D20 at the ILL at a wavelength of 2.4189 Å. A 0.3 g sample was inserted into a 5 mm vanadium can and neutron diffraction patterns were recorded at temperatures of 10, 60, and 160 K with a counting time of 4 h for each temperature. Data were also recorded at 120 K for 2 h.

The neutron diffraction patterns were all fitted by the Rietveld method¹⁶ using the GSAS program.¹⁷ The backgrounds were fitted using linear interpolation and the peak shapes were modeled using a pseudo-Voigt function. Excellent Rietveld fits ($\chi^2 \sim 2.6$, $R_{\text{WP}} \sim 1.82\%$, and $R_p \sim 1.21\%$) were obtained for all profiles using a tetragonal $I4/mmm$ structural model as previously reported for $\text{RuSr}_2\text{Gd}_{2-x}\text{Ce}_x\text{Cu}_2\text{O}_{10-\delta}$ (Ref. 18) and $\text{RuSr}_2\text{Nd}_{1.8-x}\text{Y}_{0.2}\text{Ce}_x\text{Cu}_2\text{O}_{10-\delta}$.⁸ Cell parameters were refined to $a = 3.8167(2)$, $3.8150(2)$, $3.8139(2)$, and $3.8138(2)$ and $28.429(3)$, 28.4227 , $28.413(3)$, and $28.411(3)$ at 160, 120, 60, and 10 K, respectively.

A portion of the neutron diffraction pattern obtained at 160, 120, 60, and 10 K is displayed in Fig. 4. The peak at 29.5° is the (0 0 6) nuclear Bragg peak. At 120, 60, and 10 K weak magnetic peaks are observed which can be indexed by the superlattice indices $(\frac{1}{2} \frac{1}{2} \frac{l}{2})$ with $l=1-5$ and $(\frac{1}{2} \frac{1}{2} l)$ with $l=0-2$. At a temperature of 160 K these peaks have disappeared, indicating that they are magnetic and originate from the magnetic ordering of Ru spins below 140 K (the tem-

perature at which magnetic ordering is observed in the ac susceptibility data). There is no evidence of any magnetic intensity arising from magnetic order of the Cu spins as previously reported for $\text{RuSr}_2\text{Nd}_{1.8-x}\text{Y}_{0.2}\text{Ce}_x\text{Cu}_2\text{O}_{10}$ ($0.01 \leq p \leq 0.059$) (Refs. 8 and 19) or of any magnetic diffraction from impurity phases.¹³ In contrast to the Nd-Y based materials,^{8,19} the present $\text{RuSr}_2\text{Y}_{1.5}\text{Ce}_{0.5}\text{Cu}_2\text{O}_{10-\delta}$ sample is superconducting (Fig. 1). Since superconductivity is confined to the Cu-O planes, it is clear that the Cu ions are not magnetically ordered. There is also no change in the nuclear Bragg intensity where a ferromagnetic component would appear below T_{Ru} .

Strong intraplane antiferromagnetic superexchange results in antiparallel alignment of Ru spins on the ab plane so that both a and b unit cell parameters are doubled in the magnetic supercell. The crystal structure of $\text{RuSr}_2\text{Y}_{1.5}\text{Ce}_{0.5}\text{Cu}_2\text{O}_{10-\delta}$ is body-centered tetragonal and hence all isotropic exchange interactions between the planes are canceled out. This suggests that the three-dimensional exchange observed below 140 K may be governed by weak interactions such as pseudodipolar or magnetic dipole-dipole interactions as previously observed in Pr_2CuO_4 (Ref. 20) and $\text{Sr}_2\text{CuO}_2\text{Cl}_2$,²¹ respectively. However tilts and rotations of RuO_6 octahedra have previously been observed from diffraction studies of the Ru-1222 ruthenocuprates,^{12,18} so that anisotropic interplanar exchange could also be responsible for the coupling between planes. Figure 5(a) shows three possible magnetic models. In all three models there is antiferromagnetic alignment of the Ru spins on the ab plane but a different alignment along c . In model A the spins align antiparallel along the c axis and in model B the spins align parallel along c [Fig. 5(a)]. Figure 5(b) shows that there is an unsatisfactory fit to both of these models. Magnetic diffraction from model A would result in a large intensity on $(\frac{1}{2} \frac{1}{2} \frac{l}{2})$ but negligible intensity on $(\frac{1}{2} \frac{1}{2} l)$, which is not observed experimentally, whereas magnetic diffraction from model B would result in a large intensity on $(\frac{1}{2} \frac{1}{2} l)$ and lesser intensity on $(\frac{1}{2} \frac{1}{2} \frac{l}{2})$. In order to obtain a satisfactory fit to the data, it is necessary to incorporate both parallel and antiparallel alignments of the Ru spins along c . An excellent Rietveld fit is obtained with model C [Figs. 5(a) and 5(b)], so that on average there is 50% parallel alignment along c and 50% antiparallel alignment along c . This reveals that the difference in energy between ferromagnetic and antiferromagnetic exchanges along c is negligible. The Ru moments align parallel to the c direction and the Ru moment refines to $1.5(3)\mu_B$ at 10 K. Figure 5(c) shows a portion of the neutron diffraction data between 28° and 60° 2θ , which demonstrates that the sample is phase pure and that the magnetic peaks observed do not arise from magnetic diffraction from impurity phases.¹³

The observation of a ferromagnetic moment in the sample below T_{Ru} from dc and ac susceptibility measurements may be due to the Dzyaloshinsky-Moriya (DM) (Refs. 22 and 23) spin canting mechanism, which is possible due to the tilts and rotations of the RuO_6 octahedra around c .^{12,18} Moreover weak ferromagnetism via the DM mechanism has been previously predicted to explain the magnetic properties of the 1222-ruthenocuprates.⁵ Weak ferromagnetism via the same mechanism is observed in $\text{RuSr}_2\text{GdCu}_2\text{O}_8$.⁶ Upon application of a magnetic field, the spins cant into a ferromagnetic

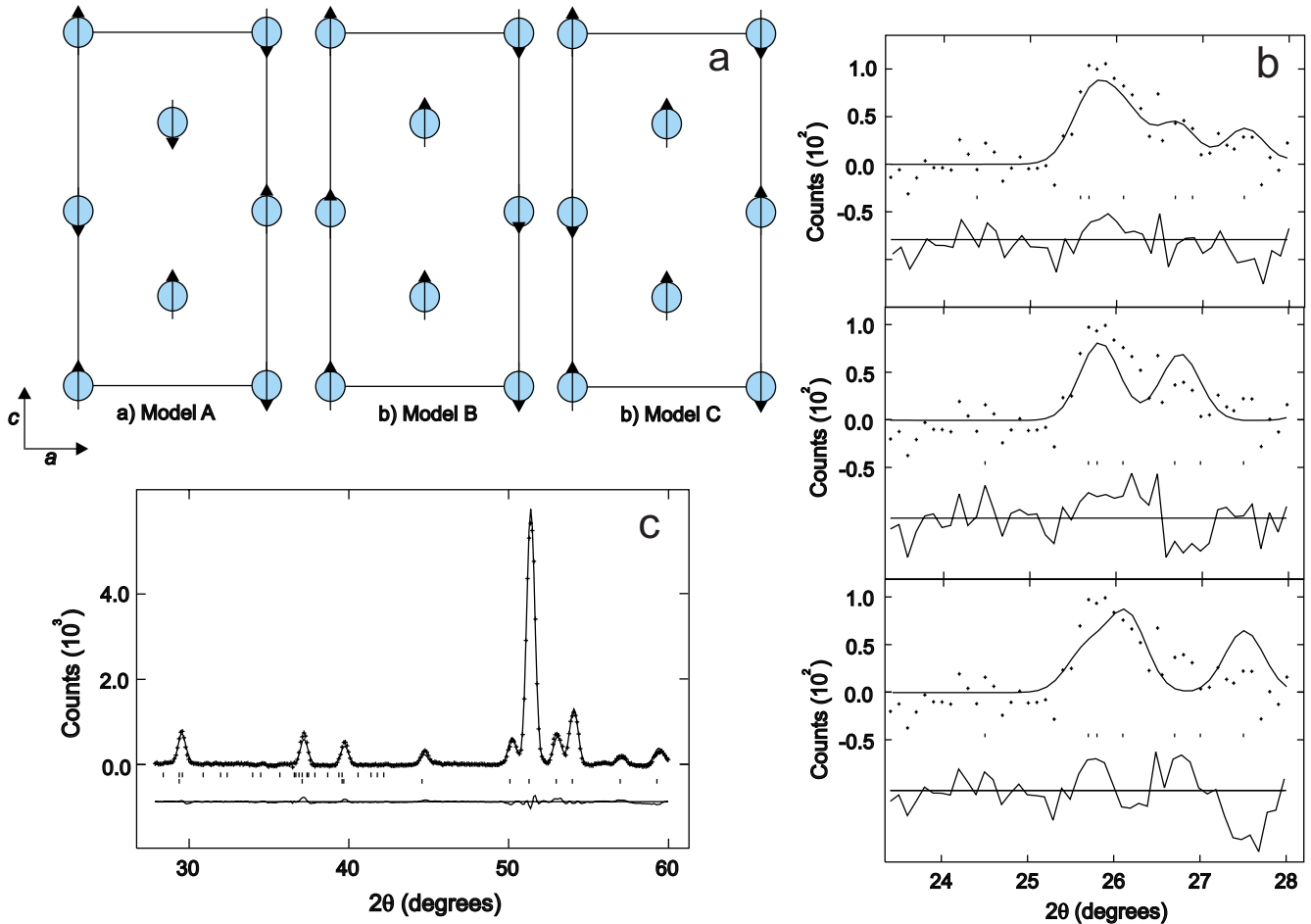


FIG. 5. (Color online) (a) The three possible magnetic structures for $\text{RuSr}_2\text{Y}_{1.5}\text{Ce}_{0.5}\text{Cu}_2\text{O}_{10-\delta}$ in which in model A the Ru moments align antiferromagnetically along c , in model B the Ru moments align ferromagnetically along c , and in model C the Ru moments in adjacent planes align antiferromagnetically and ferromagnetically along c . In all models the Ru spins align antiferromagnetically on the ab plane. Other atoms are omitted for clarity. (b) Rietveld refinement fits to models C, A, and B (from top to bottom). (c) A portion of the Rietveld refinement fit to the 10 K neutron diffraction pattern of $\text{RuSr}_2\text{Y}_{1.5}\text{Ce}_{0.5}\text{Cu}_2\text{O}_{10-\delta}$. The top and bottom reflector markers correspond to the magnetic and structural phases, respectively.

alignment on the ab plane so that by 7 T there is no significant antiferromagnetic intensity remaining. Figure 4 shows that at 120, 60, and 10 K in Ru-1222, there is no change in the nuclear Bragg intensity where a ferromagnetic component would appear below T_{Ru} within experimental error, which provides an upper limit of the ferromagnetic moment in zero field of $\sim 0.3\mu_B$. However in tetragonal symmetry, weak ferromagnetism may also arise if anisotropic pseudodipolar interactions are present between planes.²⁴ Thus it is possible that the ferromagnetic moment observed in Ru-1222 arises due to a combination of a DM exchange on the ab plane and a pseudodipolar interaction between the planes. Further studies of the interplanar interactions between Ru spins are vital in order to fully elucidate the origin of the weak ferromagnetism observed in 1222-ruthenocuprates. The variable-temperature neutron diffraction results demonstrate that there is no change in the magnetic structure upon cooling from 140 to 10 K. In contrast a peak in the ac susceptibility is observed at 91 K (Fig. 1). It has previously been suggested that upon cooling $\text{RuSr}_2\text{R}_{1.5}\text{Ce}_{0.5}\text{Cu}_2\text{O}_{10-\delta}$, an antiferromagnetic transition is observed followed by a weak

ferromagnetic transition at lower temperature.²⁵ The results from both neutron diffraction and ac susceptibility on $\text{RuSr}_2\text{Y}_{1.5}\text{Ce}_{0.5}\text{Cu}_2\text{O}_{10-\delta}$ support this theory. Thus at $T_{\text{Ru}} = 140$ K the Ru spins align in an antiparallel manner and at 91 K weak ferromagnetism is induced by canting of the Ru spins (an upper limit of the ferromagnetic moment in zero field of $\sim 0.3\mu_B$ is expected). Further neutron diffraction results in a magnetic field will be necessary to confirm this.

Previous x-ray appearance near-edge structure (XANES) studies have shown that Ru remains in the formal +5 state in the 1222-ruthenocuprates (although this is not true of 1212 types), e.g., the measured Ru valence remains at 4.95(5) as x increases from 0.5 to 1.0 in $\text{RuSr}_2\text{Gd}_{2-x}\text{Ce}_x\text{Cu}_2\text{O}_{10-\delta}$.²⁶ Ru^{5+} has the electronic configuration t_{2g}^3 so that the theoretical value for the magnetic moment is $3\mu_B/\text{Ru}$ assuming a high-spin state ($S=3/2$). In the low-spin configuration $S=1/2$ so that the theoretical magnetic moment is $1\mu_B/\text{Ru}$, which is less than the refined value of $1.5(3)\mu_B/\text{Ru}$. The theoretical value of $3\mu_B/\text{Ru}$ is considerably larger than the moment of $1.5(3)\mu_B/\text{Ru}$ refined from neutron diffraction data of $\text{RuSr}_2\text{Y}_{1.5}\text{Ce}_{0.5}\text{Cu}_2\text{O}_{10-\delta}$ at 10 K. Such a large reduction in

the moment is not uncommon in ruthenates and arises due to the strong covalency of the Ru⁵⁺-O bond, which decreases the localized moment on the Ru. The pseudo-two-dimensional nature of the magnetism will also reduce the moment due to zero-point fluctuations. However the high-temperature paramagnetic moment of $2.02\mu_B/\text{Ru}$ recorded for this sample²⁵ is much closer to the theoretical value of $1.73\mu_B/\text{Ru}$ for the low-spin state ($S=1/2$) than $3.87\mu_B/\text{Ru}$ for the high-spin state modification ($S=3/2$). It has been suggested that the assumption of completely localized moments is not adequate for RuSr₂Y_{1.5}Ce_{0.5}Cu₂O_{10- δ} .²⁵ This is further supported by the discrepancy in spin state reported here from low-temperature neutron diffraction (high spin) and high-temperature susceptibility measurements (low spin). It is also possible that a spin crossover from the high-spin to the low-spin state is observed as the temperature increases.

In conclusion results from neutron diffraction on RuSr₂Y_{1.5}Ce_{0.5}Cu₂O_{10- δ} demonstrate conclusively long-range antiferromagnetic order between Ru spins below 140 K. This is in contrast to previous neutron diffraction studies

in which there has been no evidence of antiferromagnetic Bragg peaks. These results demonstrate that the spin-glass behavior previously observed in RuSr₂Gd_{1.5}Ce_{0.5}Cu₂O_{10- δ} (Ref. 14) is not intrinsic to all 1222-ruthenocuprates and is perhaps dependent on the oxygen nonstoichiometry. The observation of a ferromagnetic moment from susceptibility measurements suggests that the Ru spins are canted below 91 K either via antisymmetric Dzyaloshinsky-Moriya exchange or by anisotropic pseudodipolar interactions between planes. Further studies of the interplanar interactions between Ru spins are necessary in order to fully elucidate the origin of the weak ferromagnetism observed in Ru-1222.

ACKNOWLEDGMENTS

The authors thank the Leverhulme Trust for financial support. This research was also partially supported by the Israel Science Foundation and by the Klachky Foundation for Superconductivity. V.P.S.A. thanks E. Takayama-Muromachi and S. Balamurugan from NIMS for his help in the sample synthesis.

*Corresponding author; a.c.mclaughlin@abdn.ac.uk

¹L. Bauernfeind, W. Widder, and H. F. Braun, *Physica C* **254**, 151 (1995).

²L. Bauernfeind, W. Widder, and H. F. Braun, *J. Low Temp. Phys.* **105**, 1605 (1996).

³C. Bernhard, J. L. Tallon, C. Niedermayer, T. Blasius, A. Golnik, E. Brucher, R. K. Kremer, D. R. Noakes, C. E. Stronach, and E. J. Ansaldo, *Phys. Rev. B* **59**, 14099 (1999).

⁴A. C. McLaughlin, W. Zhou, J. P. Attfield, A. N. Fitch, and J. L. Tallon, *Phys. Rev. B* **60**, 7512 (1999).

⁵I. Felner, U. Asaf, Y. Levi, and O. Millo, *Phys. Rev. B* **55**, R3374 (1997).

⁶J. W. Lynn, B. Keimer, C. Ulrich, C. Bernhard, and J. L. Tallon, *Phys. Rev. B* **61**, R14964 (2000).

⁷A. C. McLaughlin, J. A. McAllister, L. D. Stout, and J. P. Attfield, *Phys. Rev. B* **65**, 172506 (2002).

⁸A. C. McLaughlin, F. Sher, and J. P. Attfield, *Nature (London)* **436**, 829 (2005); **437**, 1057 (2005).

⁹A. C. McLaughlin, L. Begg, C. Harrow, S. A. J. Kimber, F. Sher, and J. P. Attfield, *J. Am. Chem. Soc.* **128**, 12364 (2006).

¹⁰V. P. S. Awana, M. A. Ansari, A. Gupta, R. B. Saxena, H. Kishan, D. Buddhikot, and S. K. Malik, *Phys. Rev. B* **70**, 104520 (2004).

¹¹A. C. McLaughlin, L. Begg, A. J. McCue, and J. P. Attfield, *Chem. Commun. (Cambridge)* **2007**, 2273.

¹²C. S. Knee, B. D. Rainford, and M. T. Weller, *J. Mater. Chem.* **10**, 2445 (2000).

¹³J. W. Lynn, Y. Chen, Q. Huang, S. K. Goh, and G. V. M. Williams, *Phys. Rev. B* **76**, 014519 (2007).

¹⁴C. A. Cardoso, F. M. Araujo-Moreira, V. P. S. Awana, E. Takayama-Muromachi, O. F. de Lima, H. Yamauchi, and M. Karppinen, *Phys. Rev. B* **67**, 020407(R) (2003).

¹⁵I. Felner, E. Galstyan, and I. Nowik, *Phys. Rev. B* **71**, 064510 (2005).

¹⁶H. M. Rietveld, *Acta Crystallogr.* **22**, 151 (1967).

¹⁷A. C. Larson and R. B. Von Dreele, Los Alamos National Laboratory Report No. LAUR-86-748, 1994 (unpublished).

¹⁸A. C. McLaughlin, J. P. Attfield, U. Asaf, and I. Felner, *Phys. Rev. B* **68**, 014503 (2003).

¹⁹A. C. McLaughlin, F. Sher, S. A. J. Kimber, and J. P. Attfield, *Phys. Rev. B* **76**, 094514 (2007).

²⁰D. Petitgrand, S. V. Maleyev, Ph. Bourges, and A. S. Ivanov, *Phys. Rev. B* **59**, 1079 (1999).

²¹D. Vaknin, S. K. Sinha, C. Stassis, L. L. Miller, and D. C. Johnston, *Phys. Rev. B* **41**, 1926 (1990).

²²I. Dzyaloshinsky, *Sov. Phys. JETP* **5**, 1259 (1957).

²³T. Moriya, *Phys. Rev.* **120**, 91 (1960).

²⁴F. C. Chou, A. Aharony, R. J. Birgeneau, O. Entin-Wohlman, M. Greven, A. B. Harris, M. A. Kastner, Y. J. Kim, D. S. Kleinberg, Y. S. Lee, and Q. Zhu, *Phys. Rev. Lett.* **78**, 535 (1997).

²⁵I. Felner, V. P. S. Awana, and E. Takayama-Muromachi, *Phys. Rev. B* **68**, 094508 (2003); I. Felner, I. Nowik, M. I. Tsindlickht, O. Yuly, I. Asulin, O. Millo, V. P. S. Awana, H. Kishan, S. Balamurugan, and E. Takayama-Muromachi, *ibid.* **76**, 144514 (2007).

²⁶G. V. M. Williams, L.-Y. Jang, and R. S. Liu, *Phys. Rev. B* **65**, 064508 (2002).